ornl

**OAK RIDGE
NATIONAL
LABORATORY**

MARTIN MARIETTA

Calculated Neutron-Induced
Cross Sections for ^{53}Cr from 1 to 20 MeV

K. Shibata
D. M. Hetrick

Engineering Physics and Mathematics Division

CALCULATED NEUTRON-INDUCED CROSS SECTIONS FOR ^{53}Cr FROM 1 TO 20 MeV*

K. Shibata** and D. M. Hetrick***

Prepared for the
Office of Basic Energy Sciences

iii

CONTENTS

CALCULATED NEUTRON-INDUCED CROSS SECTIONS FOR ^{53}Cr
FROM 1 TO 20 MeV

K. Shibata and D. M. Hetrick

ABSTRACT

Neutron-induced cross sections of ^{53}Cr have been calculated in the energy regions from 1 to 20 MeV. The quantities obtained are the cross sections for the reactions $(n,n'\gamma)$, $(n,2n)$, (n,np), $(n,n\alpha)$, $(n,p\gamma)$, (n,pn), $(n,\alpha\gamma)$, $(n,\alpha n)$, (n,d), (n,t), $(n,^3\text{He})$, and (n,γ), as well as the spectra of emitted neutrons, protons, alpha particles, and gamma rays. The precompound process was included above 5 MeV in addition to the compound process. For the inelastic scattering, the contribution of the direct interaction was calculated with DWBA.

1. INTRODUCTION

Knowledge of ^{53}Cr data is essential for evaluation of natural chromium data since the natural abundance of the isotope is 9.5%. However, experimental data on ^{53}Cr are very scarce. Thus theoretical calculations play an important role in the evaluation. In the present work, neutron cross sections of ^{53}Cr were calculated on the basis of the statistical model including precompound effects. The direct-interaction process was included for the inelastic scattering. The incident neutron energy covers the range of 1 to 20 MeV.

Two nuclear model codes were used to calculate the neutron cross sections. The statistical model code TNG[1] gave the cross sections for the reactions $(n,n'\gamma)$, $(n,2n)$, (n,np), $(n,n\alpha)$, $(n,p\gamma)$, (n,pn), $(n,\alpha\gamma)$, $(n,\alpha n)$, and (n,γ). Precompound angular distributions of neutrons from the (n,n') reaction were also calculated with the TNG code. The direct-interaction cross sections for the inelastic scattering were obtained by using the DWUCK code.[2] The angular distribution for the (n,n') reaction was generated by summing up the results of the statistical-model and direct-interaction calculations.

This report describes the details of the ^{53}Cr evaluation. In Section 2 the parameters used in the calculation are discussed. The calculated results are given in Section 3 and compared with available experimental data. A short summary is given in Section 4.

2. PARAMETERS USED IN THE CALCULATION

2.1 DISCRETE LEVELS AND LEVEL DENSITY

The statistical-model calculation was performed on the following reactions: ^{53}Cr$(n,n\gamma)^{53}$Cr, ^{53}Cr$(n,2n)^{52}$Cr, ^{53}Cr$(n,np)^{52}$V, ^{53}Cr$(n,n\alpha)^{49}$Ti, ^{53}Cr$(n,p\gamma)^{53}$V, ^{53}Cr$(n,pn)^{52}$V, ^{53}Cr$(n,\alpha\gamma)^{50}$Ti, ^{53}Cr$(n,\alpha n)^{49}$Ti, and ^{53}Cr$(n,\gamma)^{54}$Cr. The Q-values of the above reactions are given in Table 1 together with those of the (n,d), (n,t), and $(n,^3\text{He})$ reactions. In the TNG calculation, input for the discrete levels and level-density parameters of seven nuclei (i.e., ^{54}Cr, ^{53}Cr, ^{52}Cr, ^{53}V, ^{52}V, ^{50}Ti, and ^{49}Ti) are required.

Table 1. Reaction Q-values

Reaction	Q-value (MeV)
$^{53}Cr(n,2n)^{52}Cr$	−7.940
$^{53}Cr(n,np)^{52}V$	−11.134
$^{53}Cr(n,n\alpha)^{49}Ti$	−9.151
$^{53}Cr(n,p)^{53}V$	−2.640
$^{53}Cr(n,\alpha)^{50}Ti$	1.794
$^{53}Cr(n,\gamma)^{54}Cr$	9.719
$^{53}Cr(n,d)^{52}V$	−8.911
$^{53}Cr(n,t)^{51}V$	−9.965
$^{53}Cr(n,^{3}He)^{51}Ti$	−12.412

The discrete levels and gamma-ray branching ratios used in the calculation are given in Tables 2 through 8. Most of the levels were taken from the *Table of Isotopes (7th ed.)*[3] in order to be consistent with the ^{52}Cr evaluation by Hetrick et al.[4] For ^{54}Cr and ^{53}V, the recent measurements of Watson et al.[5] and Mateja et al.[6] were also taken into account. The gamma-ray branching ratios were taken from the *Table of Isotopes (7th ed.)*[3] and the *Nuclear Data Sheets.*[7] The branching ratios for primary gamma rays from ^{54}Cr are needed to calculate the capture gamma-ray spectrum and are presented in Table 9.

Concerning the level density, the composite formula of Gilbert and Cameron[8] was used throughout. The quantities a and Δ were taken from their tables except those of ^{53}Cr and ^{52}Cr. The parameters E_o and T of the constant-temperature formula and the matching energy E_x were adjusted so as to match the cumulative discrete levels of each nucleus. The parameter a for ^{53}Cr was obtained by taking account of the observed s-wave resonance spacing given by Mughabghab et al.,[9] while that for ^{52}Cr was adjusted to reproduce the measured neutron spectra from the $n + {}^{52}Cr$ reaction. For the spin cut-off factor, we used the following expression given by Facchini and Saetta-Menichella:[10]

$$\sigma^2 \equiv ct = 0.146 \, aA^{2/3}t \quad ,$$

where A is the mass number and t is the nuclear temperature. The parameters are listed in Table 10.

2.2 OPTICAL-MODEL POTENTIALS

For the optical-model potentials, we adopted the same parameters as used in the ^{52}Cr evaluation.

For neutrons, we used Wilmore and Hodgson's parameters:[11]

$$\begin{aligned}
V_R &= 47.01 - 0.267E_L - 0.0018E_L^2 & \text{(MeV)} \\
W_s &= 9.52 - 0.053E_L & \text{(MeV)} \\
r_R &= 1.322 - 7.6 \times 10^{-4}A + 4 \times 10^{-6}A^2 - 8 \times 10^{-9}A^3 & \text{(fm)} \\
r_S &= 1.266 - 3.7 \times 10^{-4}A + 2.0 \times 10^{-6}A^2 - 4 \times 10^{-9}A^3 & \text{(fm)} \\
a_R &= 0.66 & \text{(fm)} \\
a_S &= 0.48 & \text{(fm)}
\end{aligned}$$

Table 2. Discrete levels and gamma-ray branching ratios of ^{54}Cr

N	E (MeV)	$J\pi$	Branching ratios to state N		
			1	2	3
1	0.0	0 +			
2	0.835	2 +	1.0		
3	1.824	4 +		1.0	
4	2.620	2 +	0.04	0.96	
5	2.829	0 +		1.0	
6	3.074	2 +		1.0	
7	3.160	2 +		0.47	0.53
8	3.220	6 +			1.0
9	3.393	2 +		1.0	
10	3.437	2 +		1.0	
11	3.510	2 +		1.0	
12	3.660	4 +			1.0
13	3.720	1 +	1.0		

Table 3. Discrete levels and gamma-ray branching ratios of ^{53}Cr

N	E (MeV)	$J\pi$	Branching ratios to state N								
			1	2	3	4	5	6	7	8	9
1	0.0	3/2 −									
2	0.564	1/2 −	1.0								
3	1.006	5/2 −	1.0								
4	1.290	7/2 −	0.91		0.09						
5	1.537	7/2 −	0.11		0.57	0.32					
6	1.974	5/2 −	0.85			0.15					
7	2.172	11/2 −				1.0					
8	2.233	9/2 −					1.0				
9	2.321	3/2 −	1.0								
10	2.453	5/2 −			0.60	0.40					
11	2.657	5/2 −			0.72	0.28					
12	2.670	1/2 −	0.60	0.40							
13	2.707	5/2 −									1.0
14	2.708	3/2 −	0.11	0.46	0.29			0.14			

Table 4. Discrete levels and gamma-ray branching ratios of ^{52}Cr

N	E (MeV)	Jπ	Branching ratios to state N								
			1	2	3	4	5	6	7	8	9
1	0.0	0 +									
2	1.434	2 +	1.0								
3	2.370	4 +		1.0							
4	2.647	0 +		1.0							
5	2.768	4 +		0.99	0.01						
6	2.965	2 +		1.0							
7	3.114	6 +			0.99		0.01				
8	3.162	2 +	0.13	0.87							
9	3.415	4 +		0.07	0.14		0.79				
10	3.472	3 +		0.22			0.78				
11	3.616	5 +			0.54		0.42		0.03		0.01
12	3.772	2 +	0.20	0.80							
13	4.563	3 −		1.0							
14	4.640	4 +			1.0						

Table 5. Discrete levels and gamma-ray branching ratios of ^{53}V

N	E (MeV)	Jπ	Branching ratios to state N			
			1	2	3	4
1	0.0	7/2 −				
2	0.128	5/2 −	1.0			
3	0.228	3/2 −	1.0			
4	1.090	11/2 −	1.0			
5	1.265	9/2 −	0.63	0.28		0.09
6	1.550	5/2 −		0.66	0.34	
7	1.652	9/2 −	1.0			
8	1.856	7/2 −		1.0		
9	1.904	3/2 −	0.30	0.10	0.60	
10	1.958	3/2 −			1.0	
11	2.084	3/2 −		0.52	0.48	

Table 6. Discrete levels and gamma-ray branching ratios of ^{52}V

N	E (MeV)	$J\pi$	Branching ratios to state N					
			1	2	3	4	5	6
1	0.0	3 +						
2	0.017	2 +	1.0					
3	0.023	5 +	1.0					
4	0.142	1 +		1.0				
5	0.148	4 +	0.15		0.85			
6	0.437	2 +	0.49	0.30		0.21		
7	0.794	3 +					0.99	0.01
8	0.846	4 +	0.83				0.17	

Table 7. Discrete levels and gamma-ray branching ratios of ^{50}Ti

N	E (MeV)	$J\pi$	Branching ratios to state N		
			1	2	3
1	0.0	0 +			
2	1.555	2 +	1.0		
3	2.675	4 +		1.0	
4	3.200	6 +			1.0
5	3.770	2 +	0.5	0.5	
6	3.870	0 +		1.0	
7	4.160	4 +			1.0
8	4.179	2 +		1.0	

Table 8. Discrete levels and gamma-ray branching ratios of ^{49}Ti

N	E (MeV)	$J\pi$	Branching ratios to state N	
			1	2
1	0.0	7/2 −		
2	1.382	3/2 −	1.0	
3	1.542	11/2 −	1.0	
4	1.585	3/2 −	1.0	
5	1.623	9/2 −	1.0	
6	1.723	1/2 −		1.0
7	1.762	5/2 −	1.0	

Table 9. Branching ratios for primary gamma rays from the (n,γ) reaction

Final-state energy (MeV)	Branching ratio
0.0	0.15
0.835	0.46
2.620	0.08
2.829	0.02
3.074	0.10
3.437	0.02
3.720	0.04

Table 10. Level-density parameters

Residual Nuclei	T (MeV)	E_o (MeV)	a (MeV^{-1})	Δ (MeV)	c	E_c (MeV)	E_x (MeV)
^{54}Cr	1.279	0.4011	6.950	2.62	14.497	3.73	9.627
^{53}Cr	1.332	−0.789	6.500	1.35	13.39	2.772	8.306
^{52}Cr	1.433	0.1997	6.154	2.65	12.52	3.700	10.390
^{53}V	1.194	−0.556	7.200	1.27	14.83	2.360	7.433
^{52}V	1.255	−1.805	6.750	0.0	13.73	0.881	6.309
^{50}Ti	1.229	1.560	6.591	3.03	13.06	4.190	8.701
^{49}Ti	1.267	−0.2899	6.850	1.73	13.39	2.262	8.375

T = nuclear temperature

E_o = parameter for matching lower energy level density to the higher one

$a = \pi^2 g/6$ (g = density of uniformly spaced single particle states)

Δ = pairing energy correction

σ^2 = spin cut-off diameter = $2c \sqrt{(E - \Delta)/a}$ where E is the excitation energy

E_c = continuum cut-off

E_x = tangency point.

where E_L is the energy in the laboratory system and A is the mass number.

For protons, the parameters of Becchetti and Greenlees[12] were employed:

$$V_R = 54.0 - 0.32E_L + 0.4Z/A^{1/3} + 24.0(N\text{-}Z)/A \quad \text{(MeV)}$$
$$W_S = 11.8 - 0.25E_L + 12.0(N\text{-}Z)A \quad \text{(MeV)}$$
$$W_V = 0.22E_L - 2.7 \quad \text{(MeV)}$$
$$r_R = 1.17 \quad \text{(fm)}$$
$$r_S = r_V = 1.32 \quad \text{(fm)}$$
$$r_C = 1.25 \quad \text{(fm)}$$
$$a_R = 0.75 \quad \text{(fm)}$$
$$a_S = a_V = 0.51 + 0.7(N\text{-}Z)/A \quad \text{(fm)}$$

where Z is the atomic number and $N = A - Z$.

For alpha particles, the parameters of Huizenga and Igo[13] were employed:

$$V_R = 50.0$$
$$W_V = 5.7 + 0.087A$$
$$r_R = r_V = 1.17 + 1.77A^{1/3}$$
$$r_C = 1.17$$
$$a_R = a_V = 0.576$$

where W_v is based on a linear fit to the data given in Table 1 of Ref. 13.

2.3 DIRECT INTERACTION

The contribution of the direct interaction to the inelastic scattering was calculated with the DWUCK[2] code. In the calculation, the deformation parameter β_2 was required to obtain the absolute cross sections. The values of β_2's themselves were not available; thus, they were estimated from quadrupole transition probabilities $B(E2)$ which can be determined experimentally.

The probability $B(E2)$ is expressed[14] as a function of β_2 by

$$B(E2) = \frac{9}{16\pi^2} \beta_2^2 \frac{Z^2 e^2 R^4}{5} \quad ,$$

where R is a nuclear radius and e is the charge unit. For ^{53}Cr the deformation parameter β_2 is given by

$$\beta_2 = 1.4877[B(E2)]^{1/2} \quad .$$

The values of $B(E2)$'s were obtained from the compilation of Auble[7] for six levels of ^{53}Cr. The deduced β_2 values are presented in Table 11, together with β'_2 values which are used for input to DWUCK. The quantity β'_2 includes the statistical factor and is used for odd-A nuclei. It is related to β_2 by[15]

Table 11. Deformation parameters of ^{53}Cr levels

E (MeV)	J^π	L	β_2^2	β'^2_2
0.564	1/2 −	2	0.0239	0.00239
1.006	5/2 −	2	0.0215	0.00645
1.290	7/2 −	2	0.0558	0.02232
1.537	7/2 −	2	0.0055	0.00220
1.974	5/2 −	2	0.0431	0.01293
2.321	3/2 −	0	0.0328	0.03280

$$\beta'^2_2 = \frac{2J_f+1}{(2J_i+1)(2L+1)} \beta_2^2 \quad ,$$

where J_i is the spin of the target, J_f is the spin of the residual nucleus, and L is the transferred orbital angular momentum.

The calculated cross sections are shown in Fig. 1. The direct process was also taken into account for angular distributions of neutrons from the (n,n') reaction.

2.4 GIANT-DIPOLE RESONANCE

The gamma-ray transmission coefficient was calculated with the giant dipole model. The absorption cross section for giant dipole resonance was assumed to have a Lorentzian shape, i.e.,
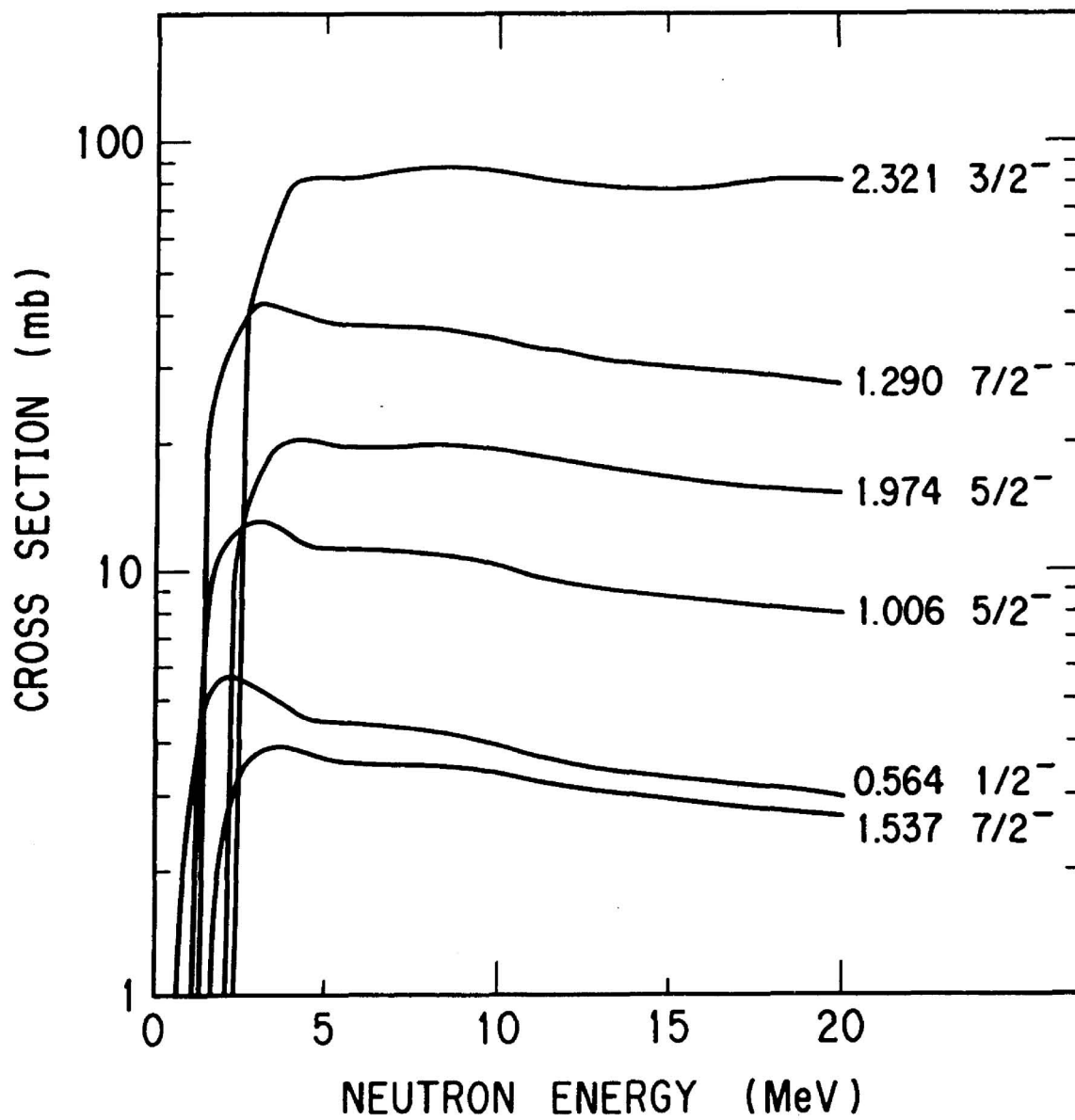
ORNL/DWG 87-8914

Fig. 1. Calculated direct inelastic scattering cross sections of ^{53}Cr.

$$\sigma^{E1}(E_\gamma) = \sigma_m \frac{E_\gamma^2 \Gamma^2}{(E_\gamma^2 - E_m^2)^2 + E_\gamma^2 \Gamma^2} \quad ,$$

where E_γ is the gamma-ray energy. The symbols E_m, σ_m, and Γ are the resonance energy, peak cross section, and full width at half maximum, respectively. Empirical formulas were used[16] to determine values of σ_m, E_m, and Γ:

$$
\begin{aligned}
\sigma_m &= 168\ NZ/(\pi A \Gamma) & \text{(mb)} \\
E_m &= 163\ (NZ)^{1/2}/A^{4/3} & \text{(MeV)} \\
\Gamma &= 5.0 & \text{(MeV).}
\end{aligned}
$$

The *M1* and *E2* transitions were also included with the assumed strengths $M1/E1 = 0.1$ at $E_\gamma = 7$ MeV and $E2/E1 = 0.01$ for all gamma-ray energies. The M_1 strength was assumed to be proportional to E_γ^3.

2.5 (n,d), (n,t), AND (n,³He) REACTIONS

The TNG code is not capable of calculating the (n,d), (n,t), and $(n,^3\text{He})$ cross sections. In the present work, these cross sections were determined from the calculated (n,p) and (n,α) cross sections by shifting the threshold energies. The absolute cross sections were obtained so that the calculated results were consistent with measured data. The experimental data used in normalization are as follows:

$(n,d) + (n,np) + (n,pn)$, 12 ± 3 mb at 14.7 MeV,   Qaim[17]

(n,t),   0.0398 mb at 14 MeV,   Qaim and Stöcklin[18]

$(n,^3\text{He})$,   0.006 mb at 14.5 MeV,   Qaim et al.[19]

In deriving the (n,d) cross section, the contributions of the (n,np) and (n,pn) reactions were estimated from the TNG calculation.

3. CALCULATED RESULTS

The calculated $(n,n'\gamma)$ cross sections are shown in Figs. 2-7, compared with two sets of measurements.[20,21] It is found that the present calculation is almost consistent with the experimental data. The inelastic scattering cross sections for the low-lying levels of ^{53}Cr are shown in Figs. 8-13, where comparisons are made with measurements[20,22] and the ^{53}Cr data of JENDL-2.[23] At higher energies JENDL-2 gives smaller cross sections than our calculations since the precompound and direct-interaction processes were neglected in JENDL-2.

No experimental data are available on the ^{53}Cr$(n,2n)$ reaction cross section. As seen in Fig. 14, the present result is 20 to 30% smaller than JENDL-2 in the energy range from 13 to 20 MeV. The $(n,2n)$ cross sections of JENDL-2 were calculated with the GROGI code[24] and adjusted to be consistent with experimental data on natural chromium.

The computed proton-production cross sections are illustrated in Fig. 15 compared with experimental data[25-30] and JENDL-2. The calculated (n,p) cross section reproduces the measurements very well, whereas JENDL-2 is inconsistent with the experimental data of Smith et al.[27] for $E_n < 9.4$ MeV.

The (n,α) and $(n,n\alpha)$ cross sections are shown in Fig. 16. In JENDL-2, the calculated (n,α) cross section was normalized to the experimental datum of Dolja et al.[31] The ^{53}Cr$(n,n\alpha)$ cross section $(MT=22)$ is not included in JENDL-2.
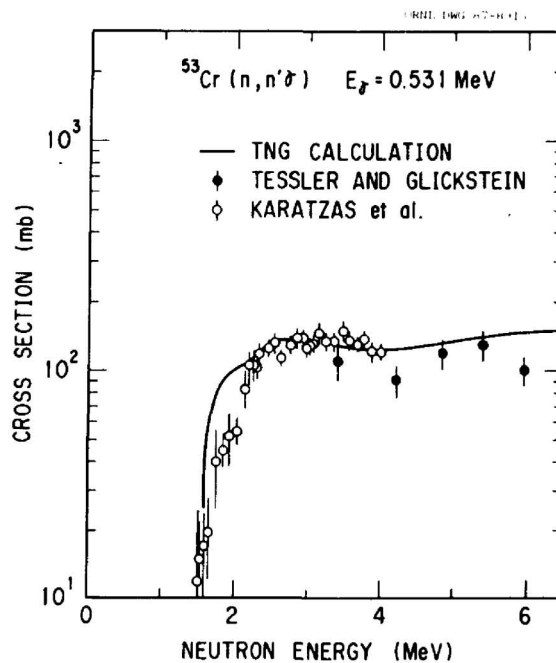
Fig. 2. Gamma-ray production cross sections for the transition from the 1.537-MeV state to the 1.006-MeV state in ^{53}Cr.
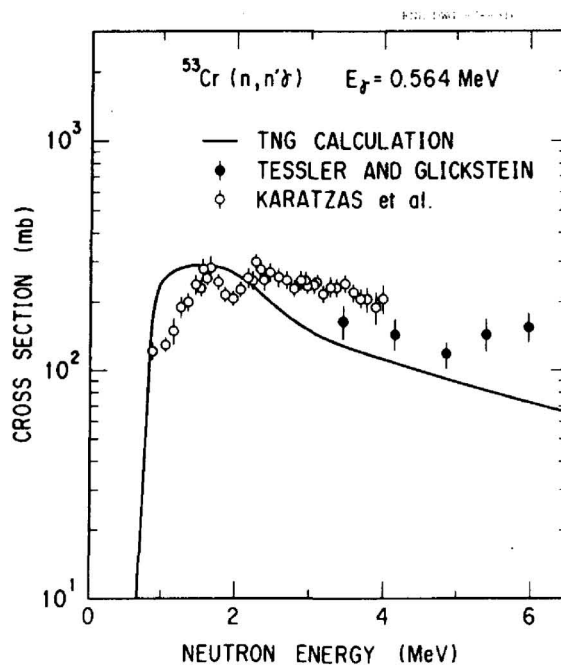

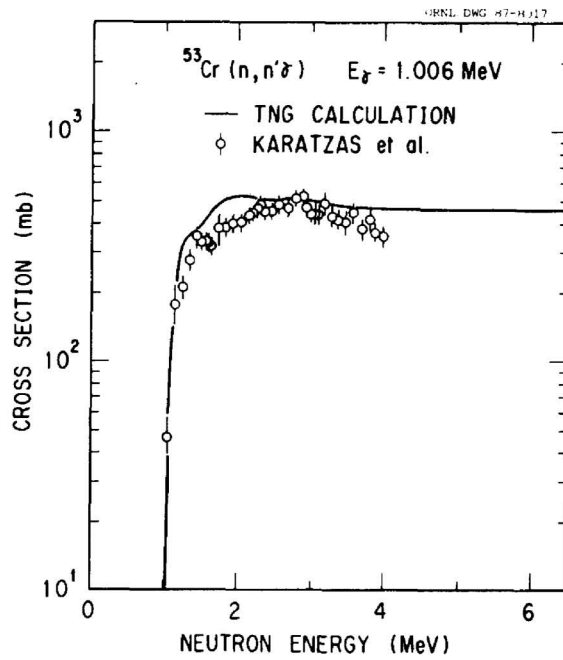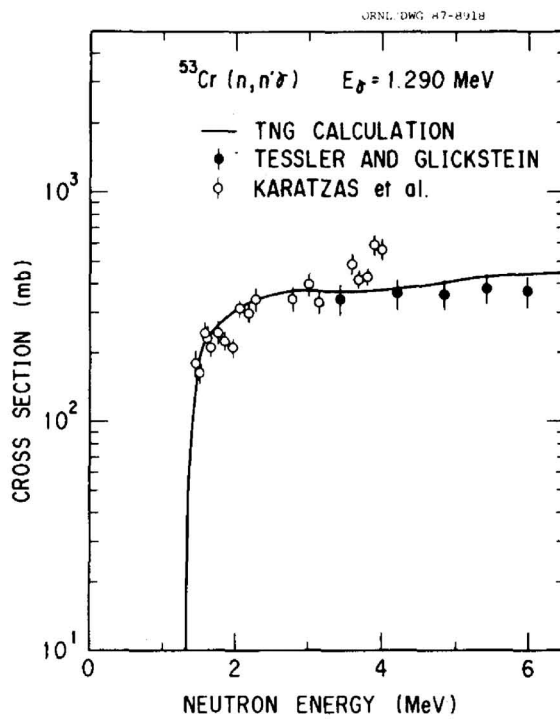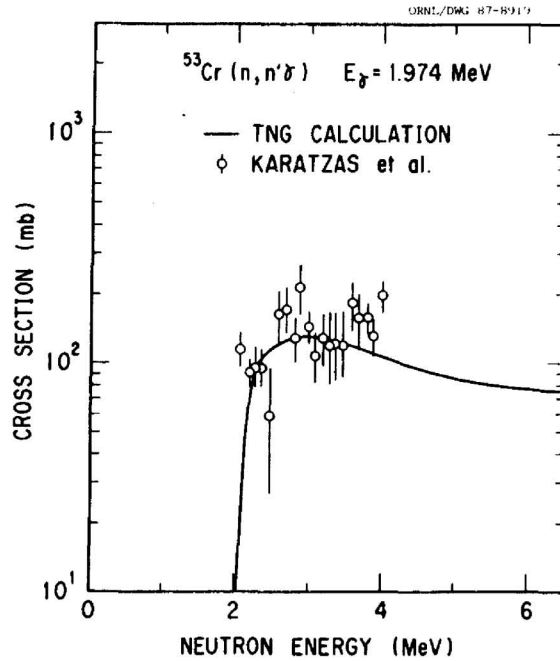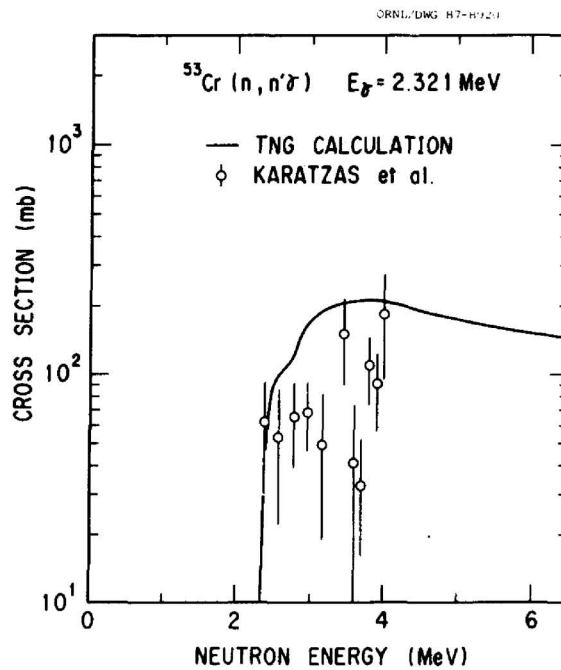**Fig. 3. Gamma-ray production cross sections for the transition from the 0.564-MeV state to the ground state in ^{53}Cr.**
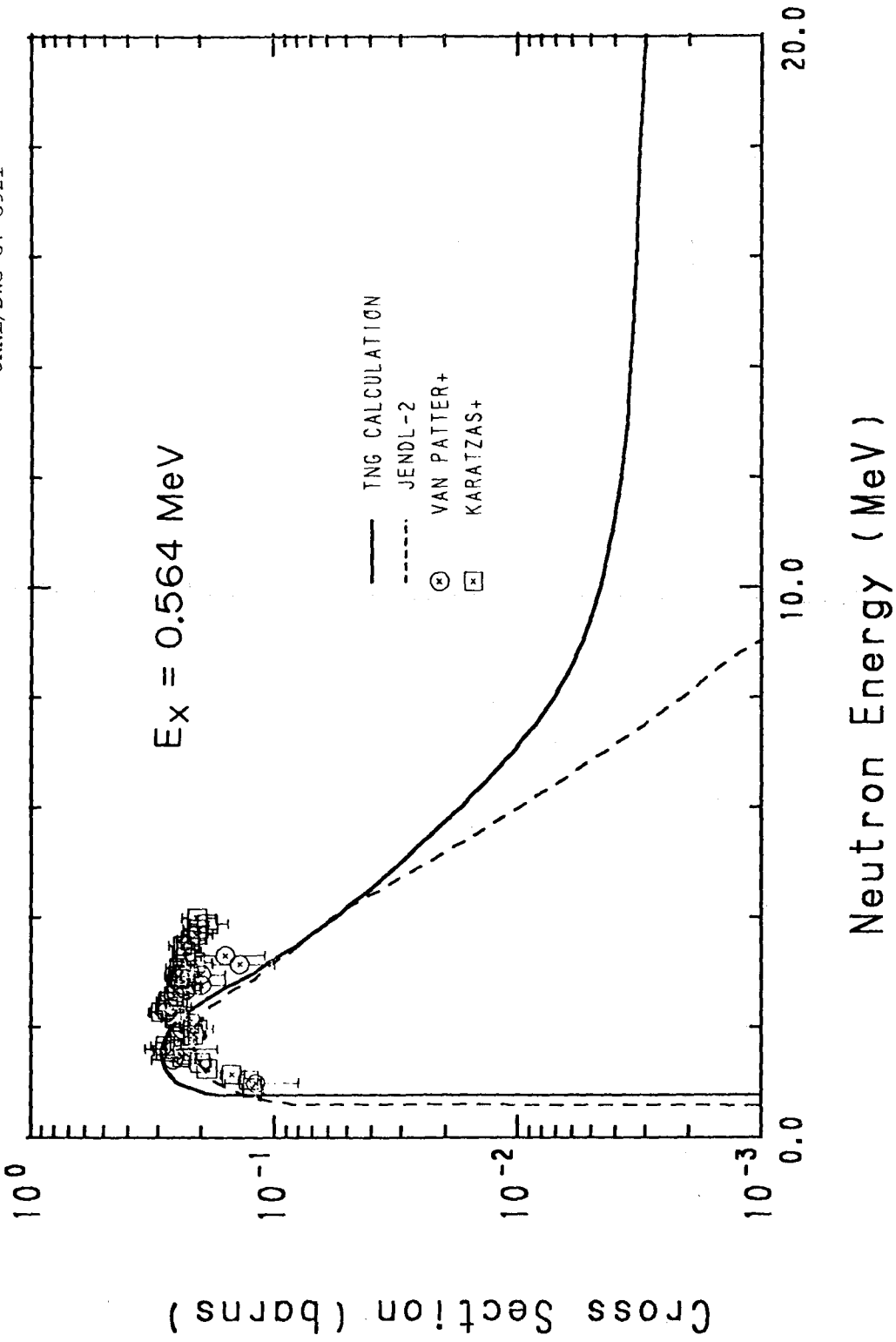
Fig. 4. Gamma-ray production cross sections for the transition from the 1.006-MeV state to the ground state in ^{53}Cr.

Fig. 5. Gamma-ray production cross sections for the transition from the 1.290-MeV state to the ground state in ^{53}Cr.

ORNL/DWG 87-8919

^{53}Cr (n, n'γ) E$_\gamma$= 1.974 MeV

— TNG CALCULATION
ϕ KARATZAS et al.

CROSS SECTION (mb)

NEUTRON ENERGY (MeV)

Fig. 6. Gamma-ray production cross sections for the transition from the 1.974-MeV state to the ground state in ^{53}Cr.

ORNL/DWG 87-8920

^{53}Cr (n, n'γ) E$_\gamma$= 2.321 MeV

— TNG CALCULATION
ϕ KARATZAS et al.

CROSS SECTION (mb)

NEUTRON ENERGY (MeV)

Fig. 7. Gamma-ray production cross sections for the transition from the 2.321-MeV state to the ground state in ^{53}Cr.

ORNL/DWG 87-8921

E_x = 0.564 MeV

TNG CALCULATION
JENDL-2
⊗ VAN PATTER+
⊠ KARATZAS+

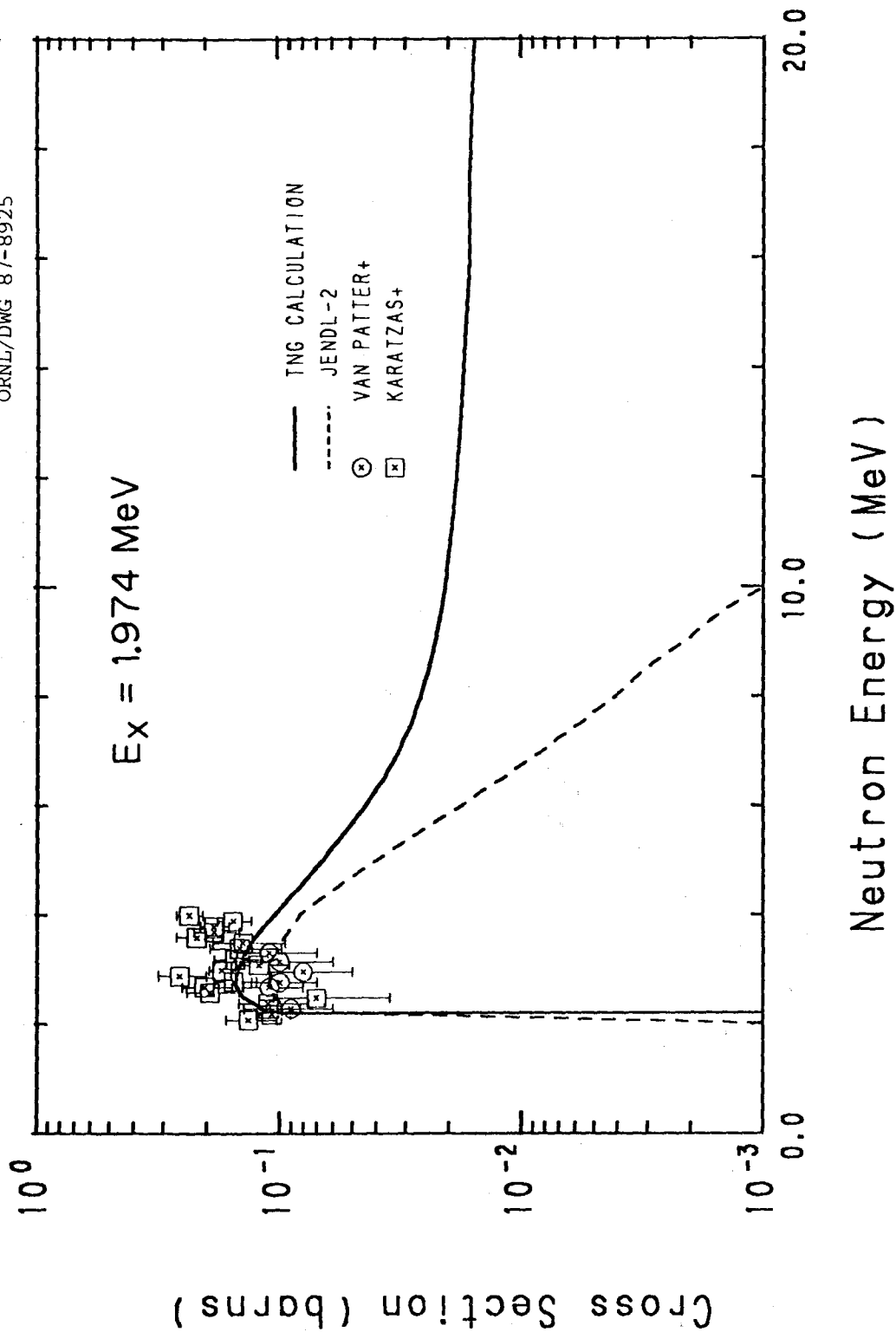Neutron Energy (MeV)

Cross Section (barns)

Fig. 8. Inelastic scattering cross sections for the 0.564-MeV state.
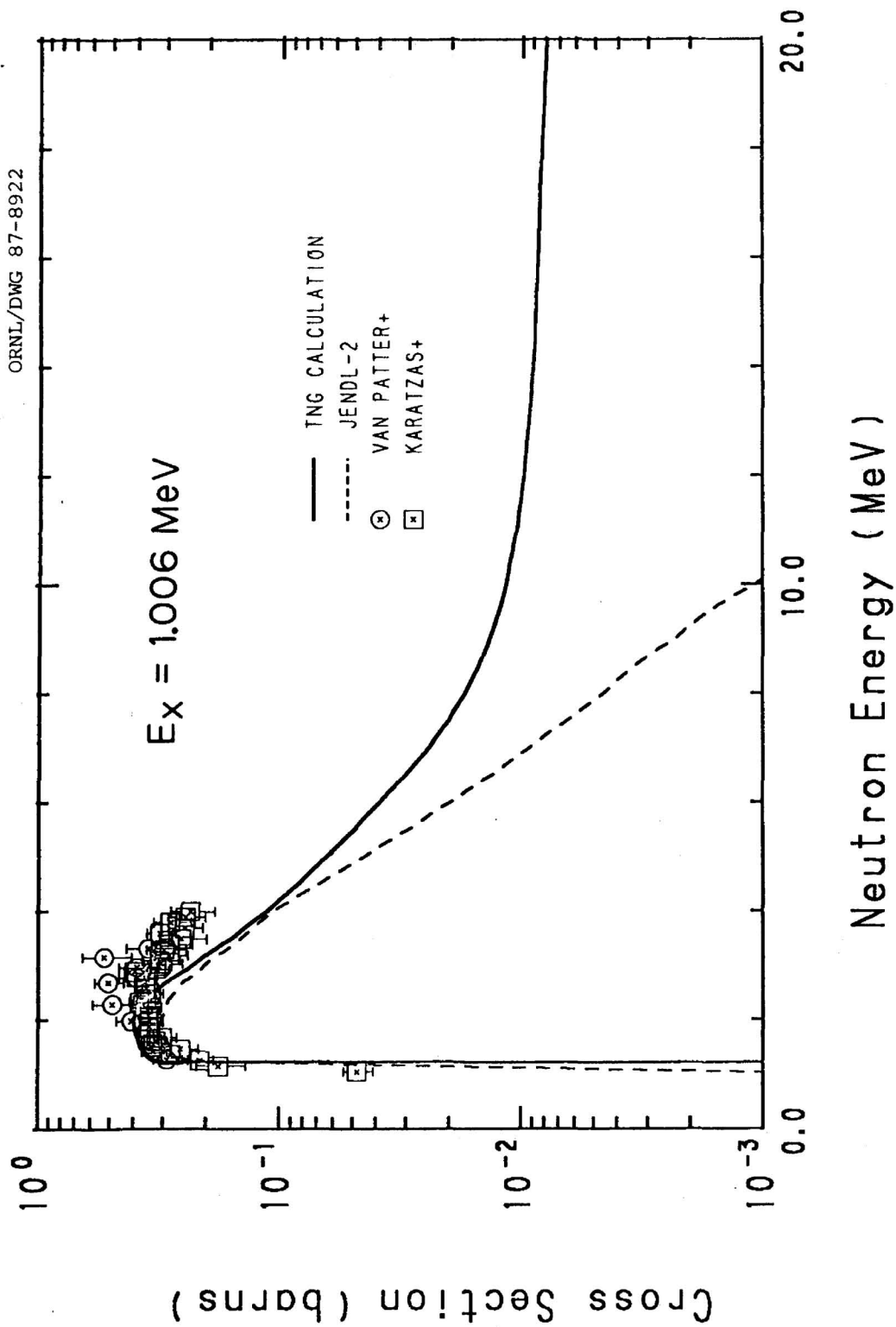
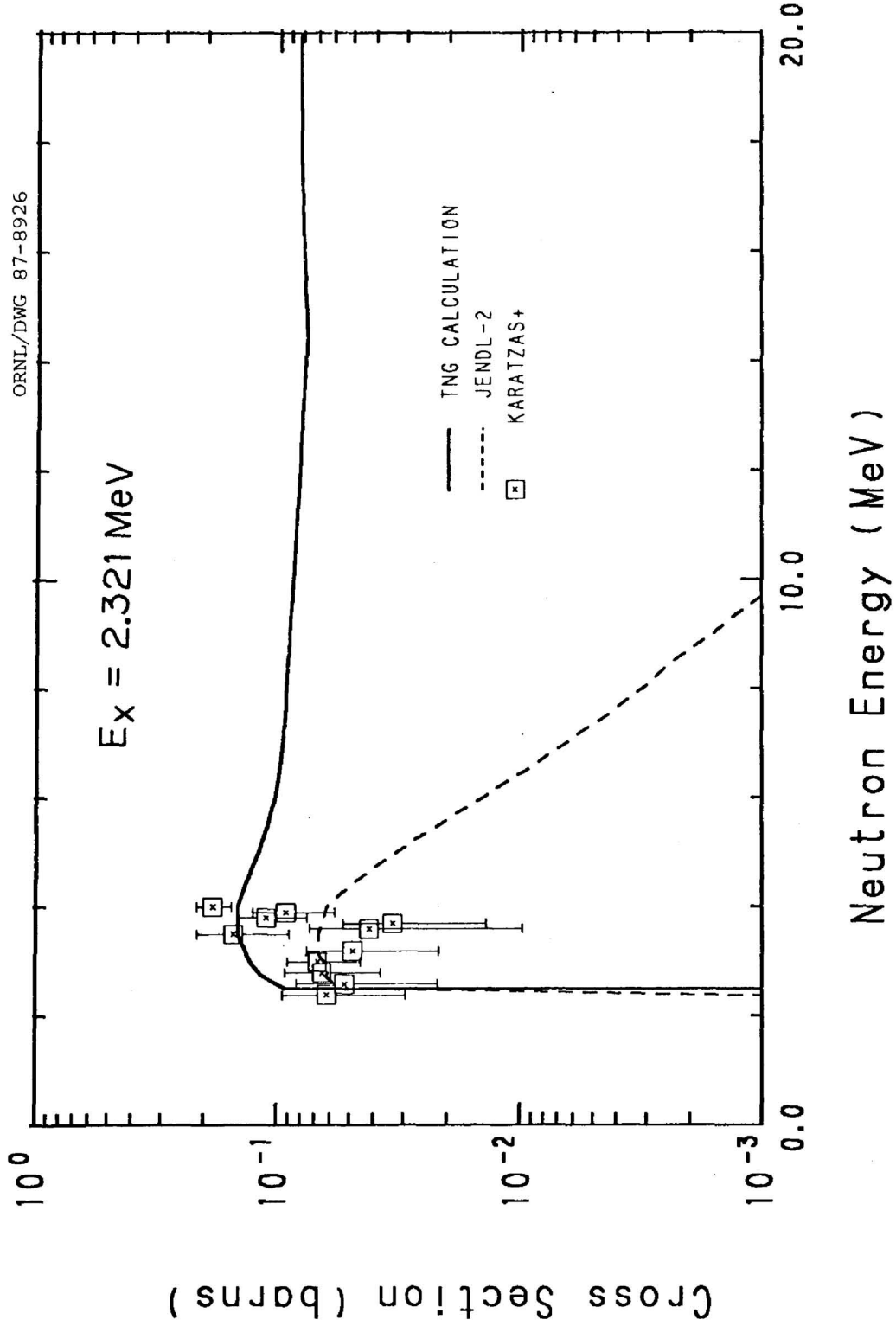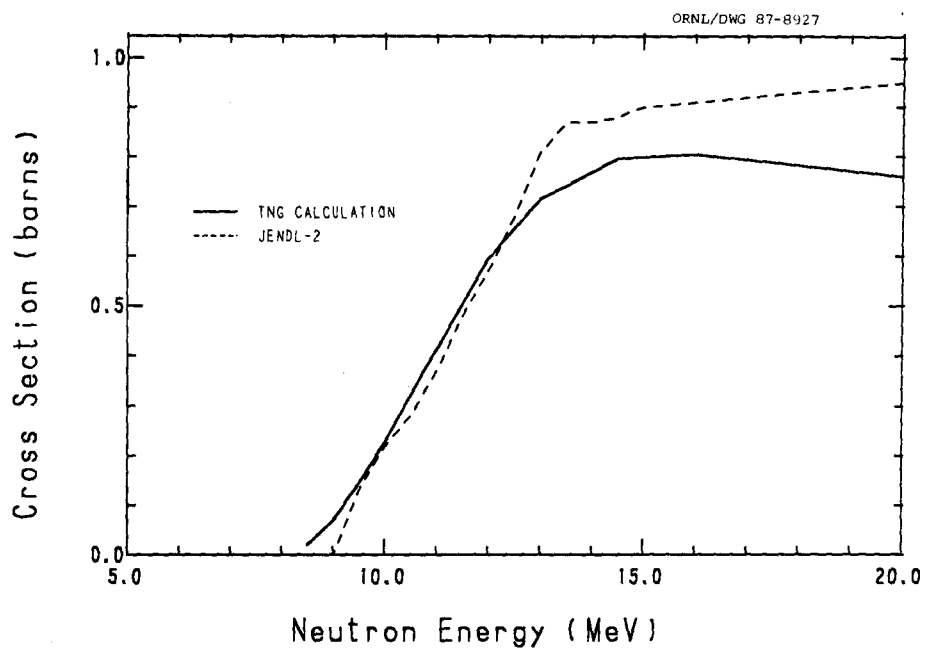**Fig. 9.** Inelastic scattering cross sections for the 1.006-MeV state.

ORNL/DWG 87-8923

E_x = 1.290 MeV

TNG CALCULATION
JENDL-2
VAN PATTER+
KARATZAS+

Neutron Energy (MeV)

Cross Section (barns)
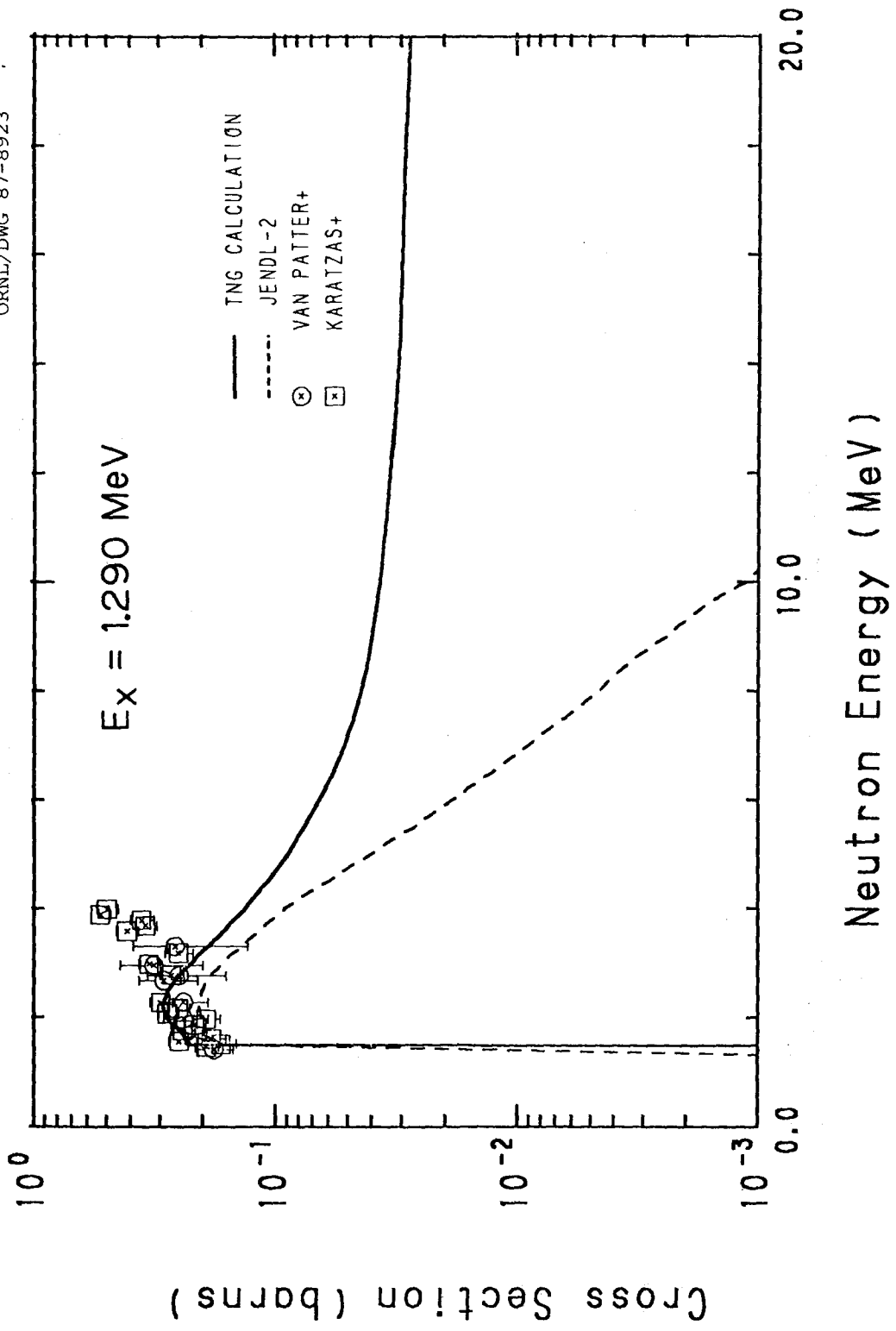
Fig. 10. Inelastic scattering cross sections for the 1.290-MeV state.
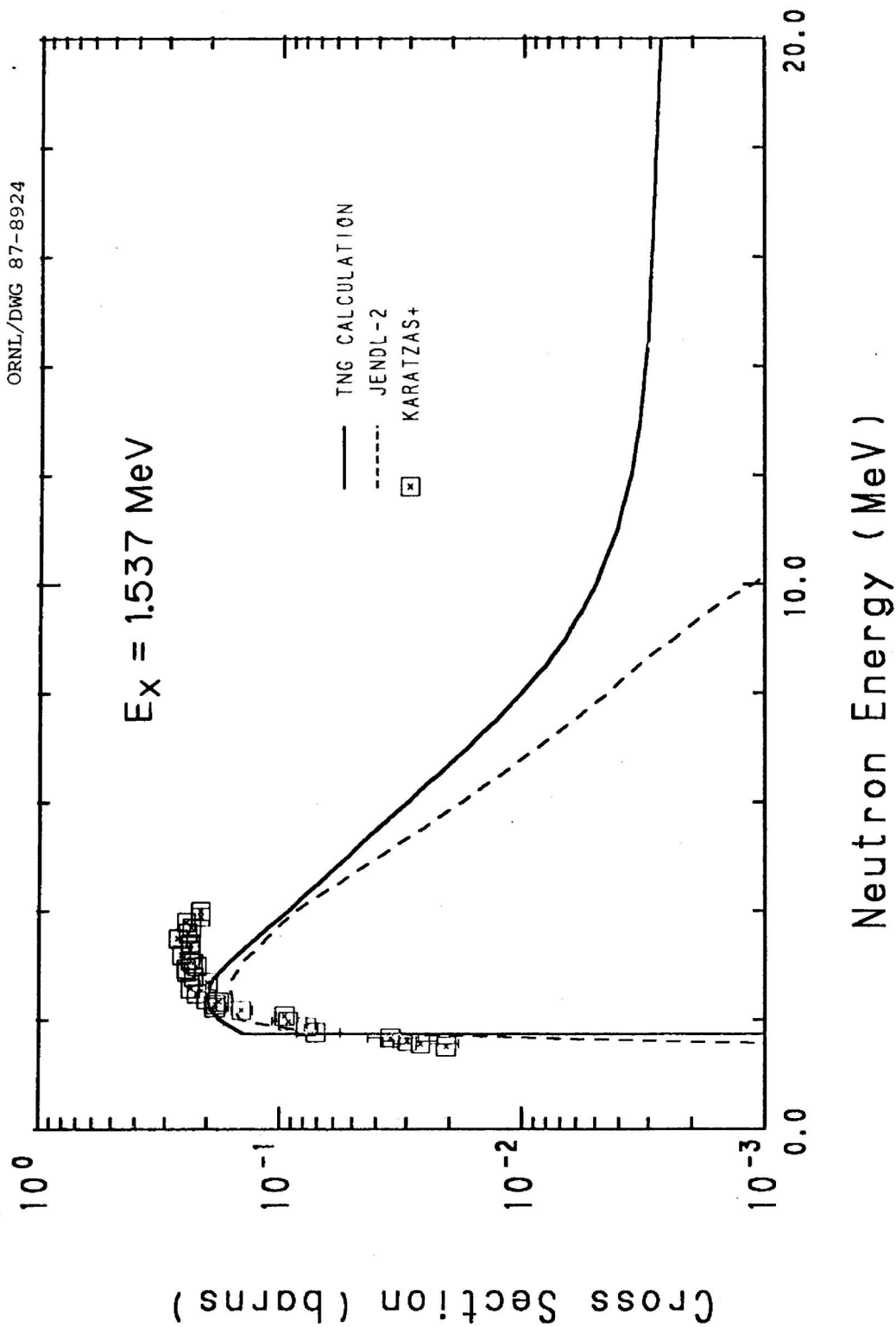
Fig. 11. Inelastic scattering cross sections for the 1.537-MeV state.

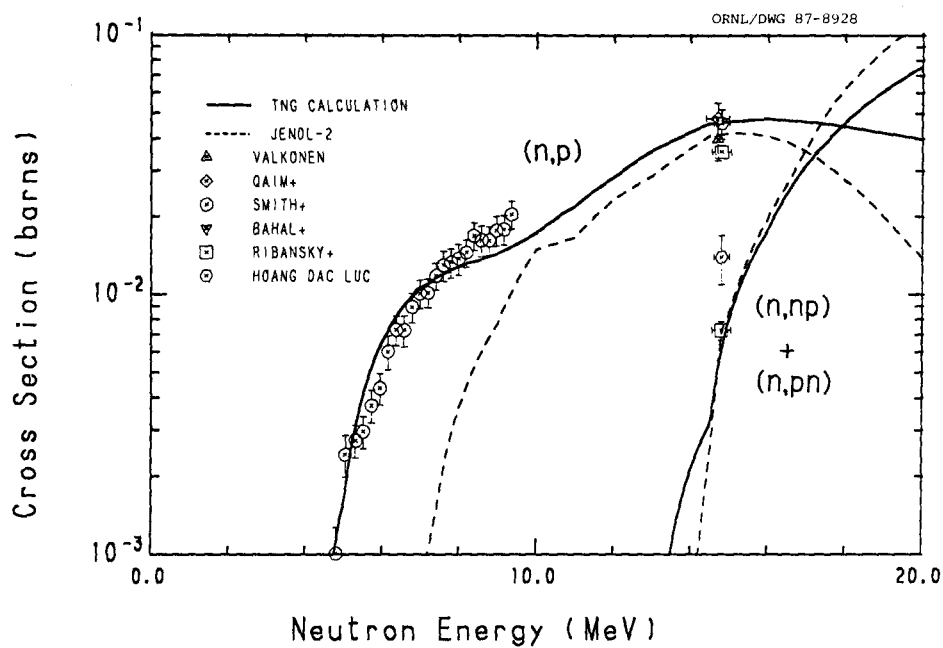Fig. 12. Inelastic scattering cross sections for the 1.974-MeV state.

ORNL/DWG 87-8926

$E_x = 2.321$ MeV

TNG CALCULATION
JENDL-2
KARATZAS+

Neutron Energy (MeV)

Cross Section (barns)

Fig. 13. Inelastic scattering cross sections for the 2.321-MeV state.

Fig. 14. (n,2n) reaction cross sections.
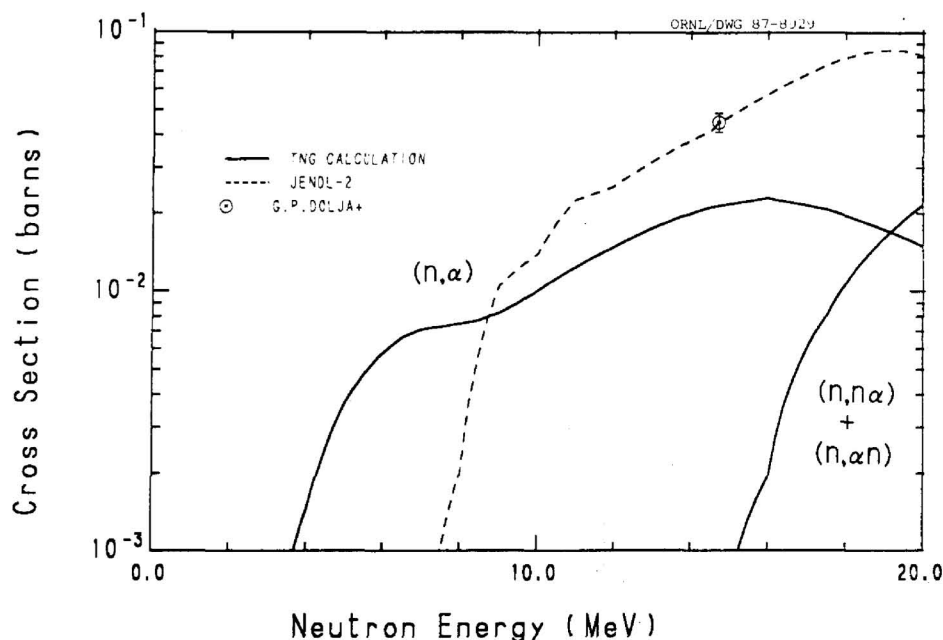

Fig. 15. Proton-production cross sections.

Fig. 16. Alpha-particle production cross sections. The JENDL-3 does not include the $(n,n\alpha)$ + $(n,\alpha n)$ component.

The capture cross section was calculated from 10 keV to 20 MeV, as shown in Fig. 17. The present result lies among the experimental data points[32-35] below 100 keV. An enhancement above 10 MeV comes from the precompound mode. Details of the precompound capture reaction are given in Ref. 36.

Shown in Fig. 18 are the (n,d), (n,t), and $(n,^3He)$ cross sections that were obtained by the method described in the previous chapter. These reaction data are not included in JENDL-2.

The spectra of emitted particles and gamma rays at an incident energy of 14.5 MeV are illustrated in Figs. 19-22. For the neutron spectrum in Fig. 19, the peak at 13 MeV is due to the direct-interaction process. Angular distributions of continuum neutrons are shown in Fig. 23. A remarkable forward peaking is seen at higher outgoing energies where the precompound reaction is predominant.

4. SUMMARY

Neutron cross sections of ^{53}Cr have been calculated in the energy range of 1 to 20 MeV. The calculations were performed using the multistep statistical model code TNG.[1] Input parameters to TNG were chosen to be consistent with those in the ^{52}Cr evaluation.[4] The resulting cross sections are consistent with available experimental data although measurements on ^{53}Cr are very scarce.

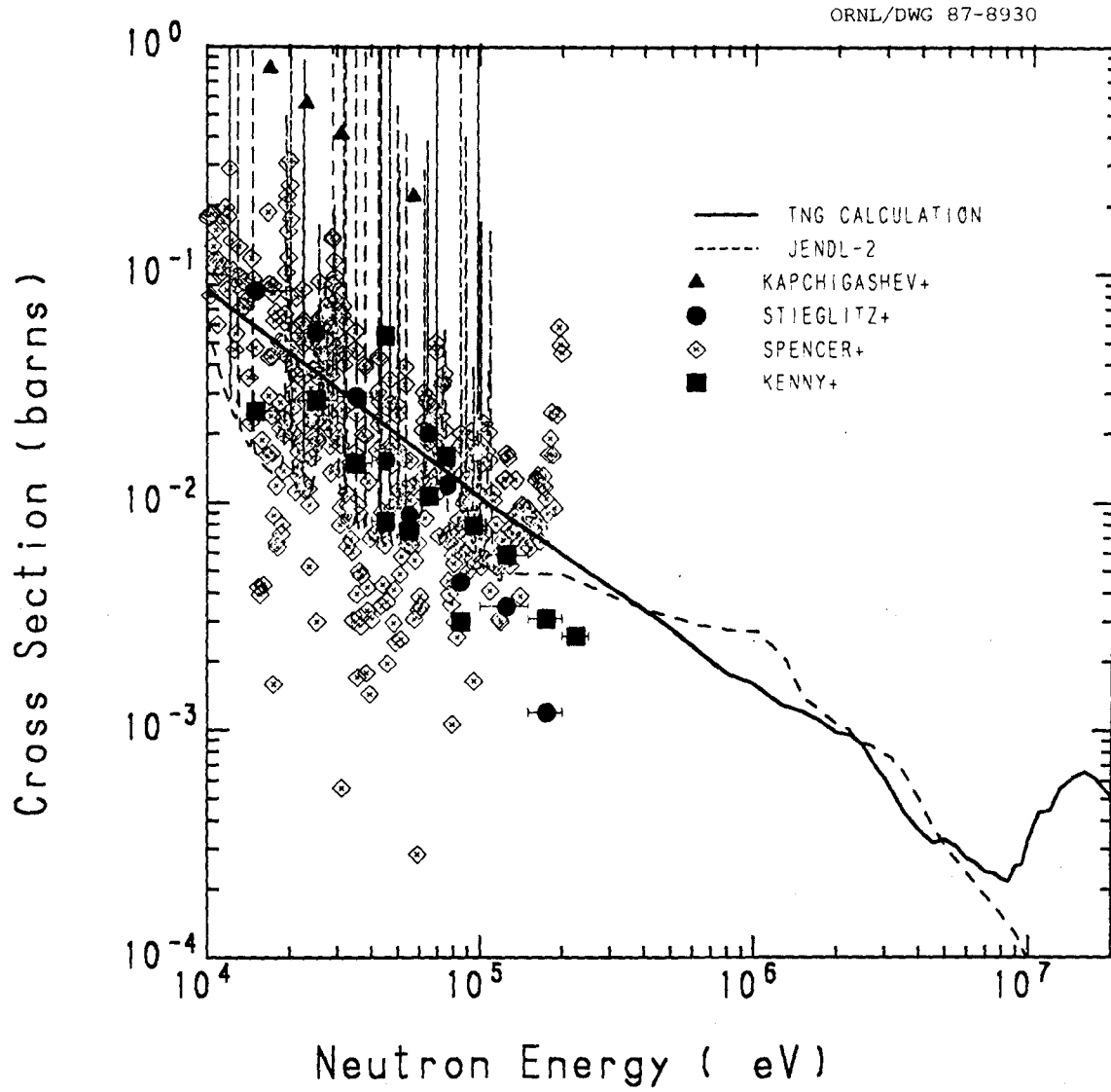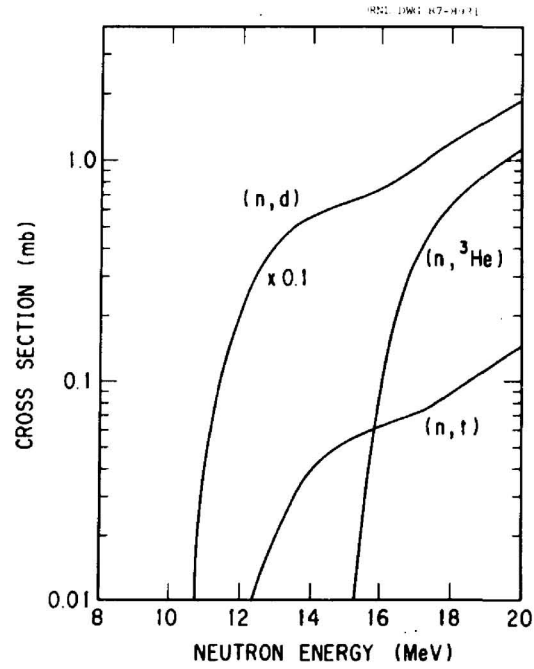Fig. 17. Radiative capture cross sections.

Fig. 18. (n,d), (n,t), and (n,^{3}He) reaction cross sections.
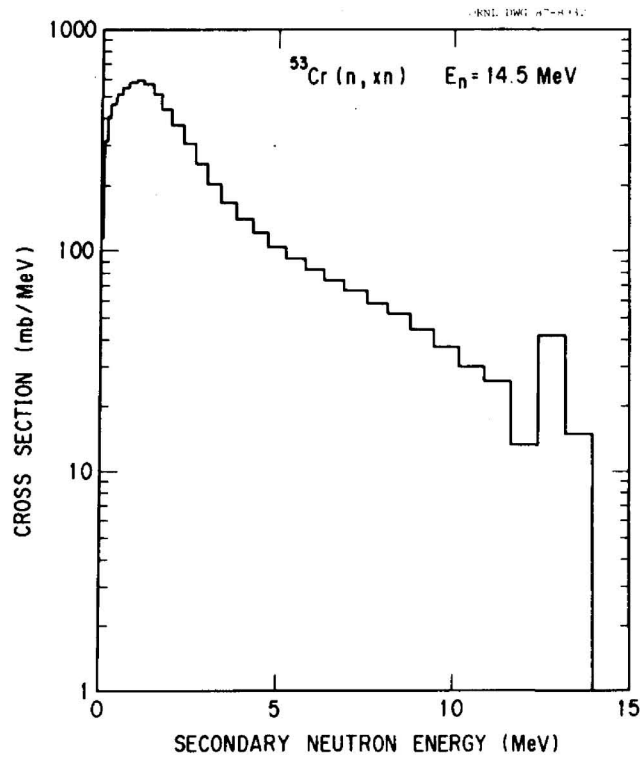

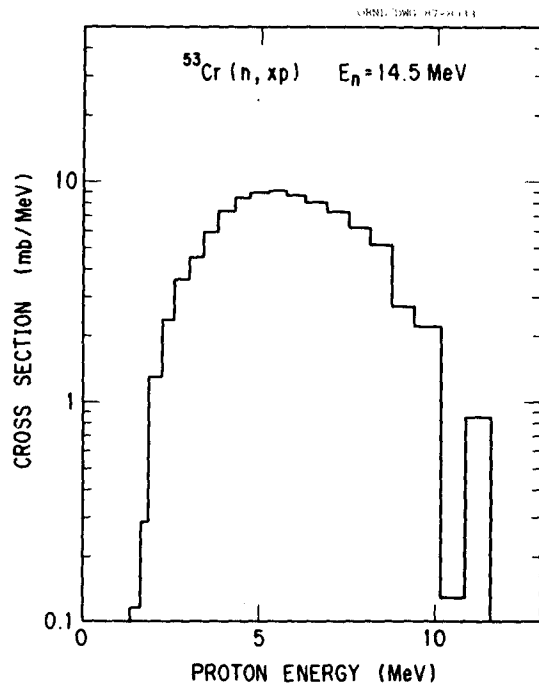**Fig. 19.** Neutron emission spectrum at an incident energy of 14.5 MeV.

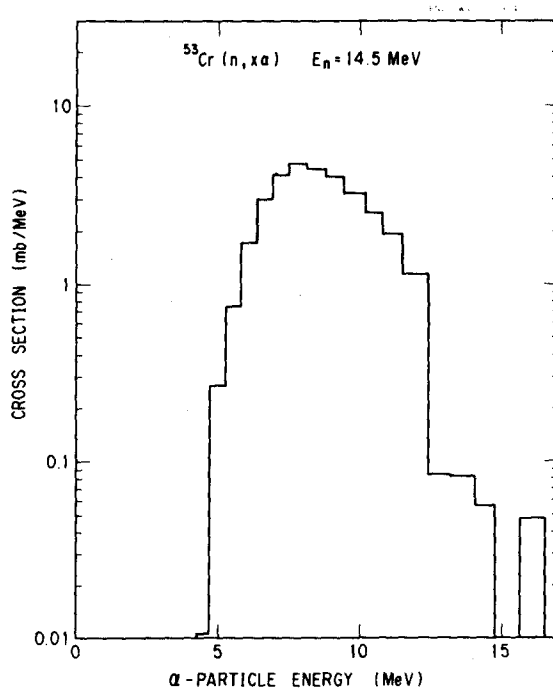Fig. 20. Proton emission spectrum at an incident energy of 14.5 MeV.

Fig. 21. Alpha-particle emission spectrum at an incident energy of 14.5 MeV.
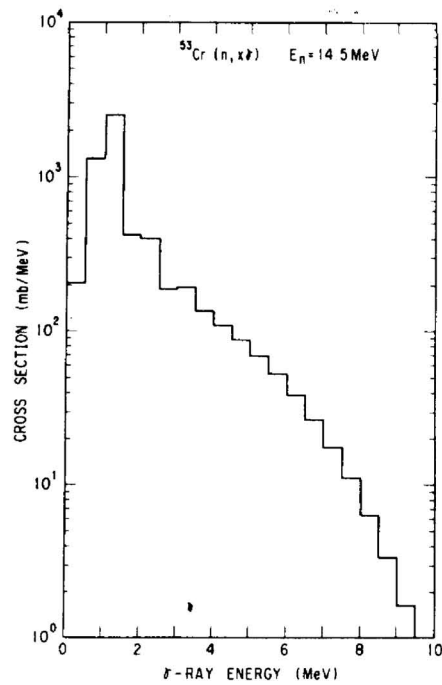
Fig. 22. **Gamma-ray emission spectrum at an incident energy of 14.5 MeV.**
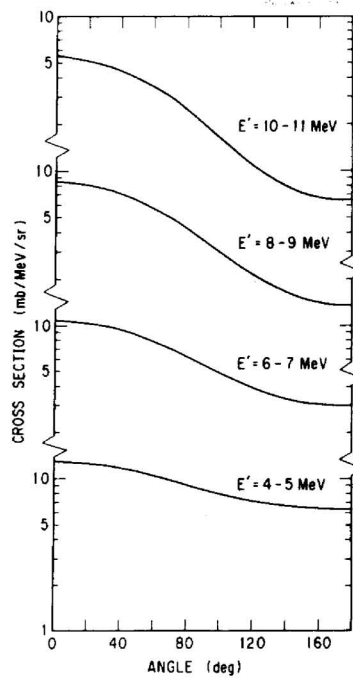

Fig. 23. **Calculated angular distributions of inelastically scattered neutrons from the ^{53}Cr(n,n') reaction at 14.5 MeV.** *E'* **stands for the outgoing energy.**

ACKNOWLEDGEMENTS

REFERENCES

1. C. Y. Fu, *A Consistent Nuclear Model for Compound and Precompound Reactions with Conservation of Angular Momentum*, ORNL/TM-7042 (1980). Also see *Nucl. Sci. Eng.* **86**, 344 (1984), *Nucl. Sci. Eng.* **92**, 440 (1986), and Ref. 36 below for revisions to the TNG code.

2. P. D. Kunz, "Distorted Wave Code DWUCK 72," University of Colorado, unpublished (1972).

3. C. M. Lederer and V. S. Shirley, *Table of Isotopes*, 7th ed., John Wiley and Sons, Inc., 1978.

4. D. M. Hetrick, C. Y. Fu, and D. C. Larson, "Calculated Neutron-Induced Cross Sections for ^{63,65}Cu, ^{58,60}Ni and ^{52}Cr from 1 to 20 MeV and Comparisons with Experiments," p. 1197 in *Proc. Int. Conf. on Nuclear Data for Basic and Applied Science, Santa Fe, 1985*, Gordon and Breach Science, 1986.

5. D. L. Watson, M. A. Abouzeid, H. T. Fortune, L. C. Bland, and J. B. McGrory, *Nucl. Phys.* **A406**, 291 (1983).

6. J. F. Mateja, L. R. Medsker, C. P. Browne, J. D. Zumbro, H. T. Fortune, R. Middleton, and J. B. McGrory, *Phys. Rev.* **C23**, 2435 (1981).

7. ^{54}Cr: H. Verheul and R. L. Auble, *Nuclear Data Sheets* **23**, 455 (1978); ^{53}Cr and ^{53}V: R. L. Auble, *Nuclear Data Sheets* **21**, 323 (1977); ^{52}Cr and ^{52}V: J. R. Beene, *Nuclear Data Sheets* **25**, 235 (1978); ^{50}Ti: R. L. Auble, *Nuclear Data Sheets* **19**, 291 (1976); ^{49}Ti: M. L. Halbert, *Nuclear Data Sheets* **24**, 175 (1978).

8. A. Gilbert and A. G. W. Cameron, *Can. J. Phys.* **43**, 1446 (1965).

9. S. F. Mughabghab, M. Divadeenam, and N. E. Holden, *Neutron Cross Sections*, Vol. 1, Academic Press, 1981.

10. U. Facchini and E. Saetta-Menichella, *Energ. Nucl.* **15**, 54 (1968).

11. D. Wilmore and P. E. Hodgson, *Nucl. Phys.* **55**, 673 (1964).

12. F. D. Becchetti, Jr. and G. W. Greenlees, *Phys. Rev.* **182**, 1190 (1969).

13. J. R. Huizenga and G. J. Igo, *Nucl. Phys.* **29**, 462 (1962).

14. A. L. McCarthy and G. M. Crawley, *Phys. Rev.* **150**, 935 (1966).

15. Yan Yiming, C. E. Brient, R. W. Finlay, G. Randers-Pehrson, A. Marcinkowski, R. C. Tailor, and J. Rapaport, *Nucl. Phys.* **A390**, 449 (1982).

16. E. G. Fuller and E. Hayward, *Nuclear Reactions*, Vol. 2, ed. P. M. Endt and P. B. Smith, North-Holland Publishing Co., p. 113 (1962).

17. S. M. Qaim, *Nucl. Phys.* **A382**, 255 (1982).

18. S. M. Qaim and G. Stöcklin, *Nucl. Phys.* **A257**, 233 (1976).

19. S. M. Qaim, S. Khatun, and R. Wölfle, *Proc. Symp. Neutron Cross-Sections from 10 to 50 MeV*, BNL-NCS-51245, p. 539 (1980).

20. P. T. Karatzas, G. P. Couchell, B. K. Barnes, L. E. Beghian, P. Harihar, A. Mittler, D. J. Pullen, E. Sheldon, and N. B. Sullivan, *Nucl. Sci. Eng.* **67**, 34 (1978).

21. G. Tessler and S. S. Glickstein, *Proc. Int. Conf. Nuclear Cross Sections and Technology, Washington, D.C., 1975*, p. 934 (1975).

22. D. M. Van Patter, N. Nath, S. M. Shafroth, S. S. Malik, and M. A. Rothman, *Phys. Rev.* **128**, 1246 (1962).

23. T. Nakagawa, *Summary of JENDL-2 General Purpose File*, JAERI-M 84-103 (1984).

24. J. Gilat, *GROGI2-A Nuclear Evaporation Computer Code Description and User's Manual*, BNL 50246 (T-580) (1970).

25. M. Valkonen, "Studies of 14 MeV Neutron Activation Cross Sections with Special Reference to the Capture Reaction," taken from *EXFOR* (1976).

26. S. M. Qaim and N. I. Molla, *Nucl. Phys.* **A283**, 269 (1977).

27. D. L. Smith, J. W. Meadows, and F. F. Porta, *Nucl. Sci. Eng.* **78**, 420 (1981).

28. B. M. Bahal and R. Pepelnik, *Cross Section Measurements of Cr, Mn, Fe, Co, Ni for an Accurate Determination of these Elements in Natural and Synthetic Samples Using a 14 MeV Neutron Generator*, GKSS-84-E (1984).

29. I. Ribansky, "Neutron Activation Cross-Sections for Cr Isotopes at 14.8 MeV Neutron Energy," taken from *EXFOR* (1985).

30. Hoang Dac Luc, "Measurement of the (n,p) and (n,np) Cross Sections on Cr Isotopes, taken from *EXFOR* (1985).

31. G. P. Dolja, V. P. Bozhko, V. JA. Golovnja, A. P. Kljucharev, and A. I. Tutubalin, "Differential and Integral Cross-Sections of (n,α) Reactions at 14.7 MeV Neutron Energy on ^{50,52,53,54}Cr Nuclei," *Proc. 2nd National Soviet Conf. on Neutron Physics, Kiev, 1973*, **3**, 131 (1974).

32. S. P. Kapchigashev and JU. P. Popov, *Atomnaja Energija* **16**, 256 (1964).

33. R. G. Stieglitz, R. W. Hockenbury, and R. C. Block, *Nucl. Phys.* **A163**, 592 (1971).

34. R. R. Spencer and H. Beer, *Capture Cross Section Measurements on Reactor Structural Materials with a Large Liquid Scintillator Detector*, KFK-2046 (1974).

35. M. J. Kenny, B. J. Allen, A. R. de L. Musgrove, R. L. Macklin, and J. Halperin, *Neutron Capture by the Chromium Isotopes*, AAEC/E-400 (1977).

36. K. Shibata and C. Y. Fu, *Recent Improvements of the TNG Statistical Model Code*, ORNL/TM-10093 (1986).

ORNL/TM-10381
ENDF-345

INTERNAL DISTRIBUTION

1.	R. G. Alsmiller, Jr.	28.	R. W. Roussin
2.	H. P. Carter/G. E. Whitesides/	29.	R. T. Santoro
	CS X-10 library	30.	R. R. Spencer
3.	J. K. Dickens	31.	P. W. Dickson, Jr. (consultant)
4-8.	C. Y. Fu	32.	G. H. Golub (consultant)
9.	T. A. Gabriel	33.	R. M. Haralick (consultant)
10-14.	D. M. Hetrick	34.	D. Steiner (consultant)
15.	J. T. Holdeman	35.	Central Research Library
16-20.	D. C. Larson	36.	Document Reference Section
21.	N. M. Larson	37.	K-25 Plant Library
22.	F. C. Maienschein	38.	Laboratory Records
23.	B. F. Maskewitz	39.	Laboratory Records - RC
24.	B. D. Murphy	40.	ORNL Patent Section
25.	M. R. Patterson	41.	EPMD Reports Office
26.	R. W. Peelle		
27.	F. G. Perey		

EXTERNAL DISTRIBUTION

42. E. D. Arthur, T-2, MS-243, Los Alamos National Laboratory, P. O. Box 1663, Los Alamos, NM 87545.

43. S. E. Berk, G234, Division of Development and Technology, Office of Fusion Energy, U.S. Department of Energy, Washington, DC 20545

44. P. Rose, Building 197D, National Nuclear Data Center, Brookhaven National Laboratory, Upton, NY 11973.

45. Chief, Mathematics and Geoscience Branch, U.S. Department of Energy, Washington, DC 20545.

46. Herbert Goldstein, 211 Mudd Columbia University, 520 West 120th St., New York, NY 10027.

47. Robert MacFarlane, T-2, MS-243, Los Alamos National Laboratory, P. O. Box 1663, Los Alamos, NM 87545.

48. F. M. Mann, W/A-4, Westinghouse Hanford, P. O. Box 1970, Richland, WA 99352.

49. G. L. Morgan, Los Alamos National Laboratory, P. O. Box 1663, Group P-15, MS D406, Los Alamos, NM 87545.

50. J. N. Rogers, Division 8324, Sandia Laboratories, Livermore, CA 94550.

51. R. E. Schenter, Westinghouse Hanford, P. O. Box 1970, Richland, WA 99352.

52. D. L. Smith, Building 314, Applied Physics Division, Argonne National Laboratory, 9700 South Cass Avenue, Argonne, IL 60439.

53-57. K. Shibata, Nuclear Data Center, Japan Atomic Energy Research Institute, Toaki Research Establishment, Tokai-Mura, Naka-Gun, Ibaraki-Ken, 319-11, Japan.

58. S. L. Whetstone, Division of Nuclear Sciences, Office of Basic Energy Sciences, U.S. Department of Energy, Washington, DC 20545.

59. P. G. Young, T-2, MS-243, Los Alamos National Laboratory, P. O. Box 1663, Los Alamos, NM 87545.

60. Office of Assistant Manager for Energy Research and Development, U.S. Department of Energy, Oak Ridge Operations, Oak Ridge, TN 37831.

61-185. April Donegain, National Nuclear Data Center, ENDF, Brookhaven National Laboratory, Upton, NY 11973.

186-215. Technical Information Center, Oak Ridge, TN 37831.